

Research Article

Research on Path Planning of Mobile Robot with a Novel Improved Artificial Potential Field Algorithm

Tiezheng Guo ¹, Jie Wang ¹, Zhiming Wang ², Wei Chen,¹ Guojun Chen ¹,
and Shishi Zhang ¹

¹Industrial Center, Nanjing Institute of Technology, Nanjing 211167, Jiangsu, China

²Key Laboratory of Crop Harvesting Equipment Technology of Zhejiang Province, Jinhua 321007, Zhejiang, China

Correspondence should be addressed to Tiezheng Guo; gtz1988@outlook.com

Received 27 May 2022; Revised 6 July 2022; Accepted 19 July 2022; Published 9 September 2022

Academic Editor: Amandeep Kaur

Copyright © 2022 Tiezheng Guo et al. This is an open access article distributed under the Creative Commons Attribution License, which permits unrestricted use, distribution, and reproduction in any medium, provided the original work is properly cited.

For the path planning and obstacle avoidance problem of mobile robots in unknown surroundings, a novel improved artificial potential field (IAPF) model was proposed in this study. In order to overcome the shortages of low efficiency, local optimization trap, and unreachable target in the classical artificial potential field (APF) method, the new adaptive step length adjustment strategy was proposed in IAPF, which improved the path planning and obstacle avoidance efficiency. A new triangular navigation method was designed to solve the local optimization trap in joint force zero condition for a variety of path planning. In order to solve the target unreachable problem, a new target attraction model was established based on the distance of obstacle to improve convergence rate, and the new method was designed such as adding the aim factor to optimize the rejection force function and so on. The two methods of IAPF and APF are compared using MATLAB simulation, the average path planning efficiency of IAPF is increased by 42.8% compared with APF, the average path length is reduced by 8.6%, and the average target convergence rate is increased by 26.1%. Finally, the physical test of the mobile robot verified the effectiveness and accuracy of IAPF.

1. Introduction

Due to the rapid development of industrial automation and intelligence, as well as the constant improvement of human living conditions, the use of robots has become more and more extensive and has gradually become an indispensable part of human production and life. Motion planning technology has received widespread attention as a necessary link in the robot's intelligent autonomous operation [1].

In recent years, a large number of research results have been achieved in the path planning of mobile robots. The conventional methods have been widely used such as the grid method [2], A* algorithm [3], and artificial potential field method [4]. In order to adapt mobile robots to different application fields and complex and changing industrial environments, various intelligent algorithms have emerged to provide new solutions for mobile robot path planning. The commonly used intelligent algorithms include genetic algorithm [5, 6], particle swarm algorithm [7], and neural network algorithm [8], as well as the proposed fusion and

improvement based on the above algorithms. Among them, compared with other algorithms that have met some problems of the long computing time, poor real-time obstacle avoidance, and many iterations under some special circumstances, the artificial potential field method has a simple structure, small computation, fast response time, low hardware platform requirements, and easy underlying real-time control, and is widely used in real-time obstacle avoidance and smooth trajectory control.

Although it has many advantages, the classical APF method also has some defects, such as inaccessible target and easy to fall into local optimum [9]. Scholars have conducted several research in effort to address this issue. For example, a novel repulsive potential function was presented by Azzabi and Nouri [10]. When a robot is locked in a local minimum, the escape force is activated to assist the robot in breaking free from the stalemate position and turning gradually away from the obstacles in order to solve the local minimum problem. Rostami et al. [11] proposed a virtual target point, which creates a pulling force to assist the robot in escaping

when the robot falls into a local optimal state. Batista et al. [12] proposed a virtual obstacle model and modified the repulsion function to solve target unreachable problems in the planning algorithm. However, the algorithm used the equal-step path method and the overall planning efficiency was not high. Jung and Kim [13] used the tangent method to solve the local minimum problem formed by multiple obstacles and introduced a target factor to overcome the problem of the unreachable target. However, when there are multiple obstacles in front of the target point, the convergence speed of the robot is slow. Pashna et al. [14] improved the target unreachable and local minimum defects in the classical APF method, introduced a target distance factor, modified the repulsive force function in potential field, and solved the target unreachable problem. The deflection angle method was used to construct the traction force for solving the local minimum problem, but when escaping from the local minimum point of multiple obstacles, the planned path appears jagged and the path curve was not smooth obviously enough.

Based on the existing research and problems met, the novel improved artificial potential field (IAPF) path planning model in multiobstacles complex environment was proposed in this study. A new triangle navigation method was designed to establish a planning guide point when the mobile robot fell into a local optimal situation and used the additional attraction force of the guide point to get away from the local minimum value and solve the local optimal problem; An adaptive step length adjustment strategy was proposed to dynamically adjust step length according to the number of obstacles, so as to improve the planning efficiency of the system. A new target attraction model based on obstacle distance was built to improve the target convergence speed, and the target distance factor was added to optimize the repulsion function to address the problem of a nonreachable goal.

The structure of this study is organized as follows: Section 2 is mainly about the existing problems in the classical APF model. In Section 3, the corresponding improvement measures are proposed and a novel IAPF model is established. Demonstration of the effectiveness and superiority of the IAPF algorithm through simulation and algorithm comparison is illustrated in Section 4. Physical tests verifying the effectiveness and accuracy of the IAPF are introduced in Section 5. Finally, the conclusions are presented in Section 6.

The main contributions of this study are as follows:

- (i) Aiming at the optimal path planning problem of mobile robots in unknown surroundings, a unique IAPF model was proposed, which overcomes the problems of the classical APF method, such as low efficiency in algorithm planning, easy to trap local optimum, and unreachable target.
- (ii) A novel triangular navigation method was designed to solve the local optimization trap in joint force zero condition for a variety of path planning. The new adaptive step length adjustment strategy was

designed to improve the efficiency of path planning and obstacle avoidance.

- (iii) The target attraction model based on the distance of obstacles was built to improve the algorithm convergence speed, and the repulsion function was optimized by adding the target factor to solve the target unreachable problem.

2. Classical Artificial Potential Field Method

The basic idea of the APF method [15] is similar to the "electromagnetic field," which regards obstacles as repulsive points and targets as attractive points to construct repulsive and attractive potential fields. Obstacles and targets respectively generate repulsive force F_{rep} and attractive force F_{att} on the mobile robot. The mobile robot's movement, path planning, and real-time collision avoidance are all guided by the joint force F . The working principle is shown in Figure 1.

In order to calculate the attractive and repulsive forces received by the mobile robot, first, the attractive field function and repulsive field function are defined [16]. By taking the negative gradient of the two potential field functions, the attractive and repulsive functions are obtained. The classical functions of attractive field U_{att} and repulsion field U_{rep} are as follows:

$$U_{att} = \frac{1}{2} \mu q g^2 \vec{q}_g, \quad (1)$$

$$U_{rep} = \begin{cases} \frac{1}{2} \sigma \left(\frac{1}{q_{obs}} - \frac{1}{d_{obs}} \right)^2 \vec{q}_{obs}, & 0 \leq q_{obs} \leq d_{obs}, \\ 0, & q_{obs} > d_{obs}, \end{cases} \quad (2)$$

where μ is the attractive gain coefficient, σ is the repulsion gain coefficient, q_g is the distance between the current position of the robot and the target point, \vec{q}_g is the unit vector of the current position of the robot pointing to the target point, q_{obs} is the distance between the current position of the robot to the obstacle, \vec{q}_{obs} is the unit vector of the robot's current position pointing to the obstacle, and d_{obs} is the action distance of repulsive field of obstacle.

The corresponding attractive function F_{att} and repulsive function F_{rep} are as follows:

$$F_{att} = -\nabla U_{att} = -\mu q_g \vec{q}_g, \quad (3)$$

$$F_{rep} = -\nabla U_{rep} = \begin{cases} \sigma \left(\frac{1}{q_{obs}} - \frac{1}{d_{obs}} \right) \frac{1}{q_{obs}^2} \vec{q}_{obs}, & 0 \leq q_{obs} \leq d_{obs}, \\ 0, & q_{obs} > d_{obs}. \end{cases} \quad (4)$$

The formula of the joint force on the robot is as follows:

$$F = F_{att} + \sum_1^n F_{rep}, \quad (5)$$

where n is the number of obstacles.

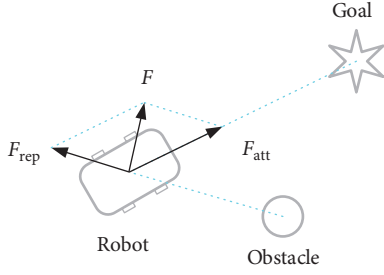


FIGURE 1: Schematic diagram of potential field.

In robot route planning and obstacle avoidance, the traditional APF approach is commonly employed. However, when it is tested in a complex unknown environment, the following problems are encountered: (i) APF adopts an equal step planning method, which cannot be fully applied in multiple obstacles environment, and the algorithm efficiency needs to be improved. (ii) When the joint force of the mobile robot is zero, the planning algorithm loses the next forward direction and the system falls into a local optimal state. (iii) When there are obstacles near the target point, the repulsion force is greater than the attractive force when the mobile robot reaches the target point, which causes the mobile robot to oscillate near the target point, the convergence speed is slow, and even cannot reach the target point.

3. Improved Artificial Potential Field Model

In the study, to solve the problems of the classical APF method in the path planning of mobile robot applicable to the complex unknown environments, the corresponding improvement methods are proposed and novel models are established from the following three aspects.

3.1. Adaptive Step Length Adjustment Method. The classical APF method adopts the equal step length in the path planning method, which has the problems of low efficiency and long operation time and cannot be fully applied in a complex unknown environment. The actual test shows that in the simple environment with a small number of obstacles, the step length can be appropriately enlarged so as to reduce the path points to be calculated and accelerate the robot moving speed, which leads to improve the efficiency of path planning and reduce the system operation time. In the complex environment with multiple obstacles, the robot moving speed can be decelerated by appropriately reducing the step length, so as to reduce the collision probability.

Based on the number of obstacles, the distance between robot and obstacle, and iteration times, an adaptive step length adjustment method is proposed and expressed as follows:

$$\text{step} = \rho \frac{1}{n} * 2 \sqrt{q_{\text{obs}}/d_{\text{obs}}} * e^{(c/c_{\text{max}})^2}, \quad (6)$$

where ρ is the step gain coefficient, c is the current iteration time, and c_{max} is the upper limit of iterations.

According to formula (6), step length is inversely proportional to the number of obstacles, so the more obstacles there are, the smaller step length is. Step length is proportional to the distance that from robot to obstacle, the closer the robot is to the obstacle, the smaller the step length and the lower the collision risk. Step length is proportional to the number of iterations, the more iterations, the larger the step length and the faster the target convergence rate.

3.2. Triangular Navigation. In the operation process of mobile robot, there are mainly two cases for the local optimal problem: (i) due to the scope of the obstacles potential field, it may happen that only one single obstacle potential field produces repulsion, and its direction is collinear with the attractive direction, which leads to the mobile robot wandering in the current position. When the joint force is zero, the robot stops moving. (ii) When the mobile robot encounters multiple obstacles, the repulsion force and attractive force are collinear, which leads to the mobile robot wandering in the current position. When the joint force is zero, it stops moving. The two cases are shown in Figure 2.

In view of the above two cases, the triangle navigation method is proposed to solve the local optimal problem in this study. The following two cases are discussed respectively.

3.2.1. Single Obstacle. The move direction of the mobile robot is provided by the joint force in the path planning. When the repulsion force and attractive force are collinear, the mobile robot oscillates back and forth or stops moving in the current position, so the extra force is needed to make the mobile robot escape from the local optimum. The solution is to use the triangle navigation method to determine the guidance point, which provides an attractive force to guide the robot escape from the local area. Figure 3 shows the triangle navigation method in a single obstacle condition.

As shown in Figure 3, $O(x, y)$ is the obstacle coordinate, $G(x, y)$ is the guidance point coordinate, and $P(x, y)$ is the current position coordinate of the robot. With the obstacle as the center of the circle and the safe distance d as the radius of the circle, the line perpendicular to straight line of connecting the obstacle and the robot that intersects the circle at point G is made, and guiding point G provides additional attraction F_{att} to help the robot escape from the local optimum.

The guide point calculation formula is as follows:

$$\begin{cases} \sqrt{(G_x - O_x)^2 + (G_y - O_y)^2} = d, \\ \frac{G_y - O_y}{G_x - O_x} \frac{O_y - P_y}{O_x - P_x} = -1. \end{cases} \quad (7)$$

According to the known obstacle coordinates $O(x, y)$ and the robot's current position coordinates $P(x, y)$, the guiding point $G(x, y)$ can be obtained by formula (7).

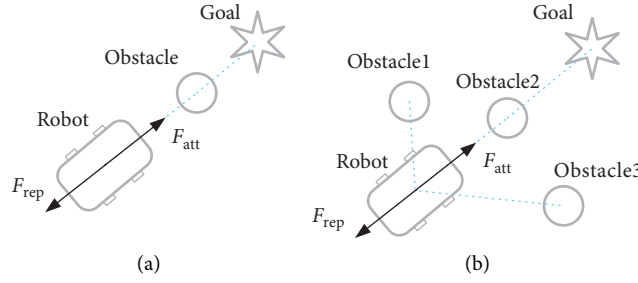


FIGURE 2: Local optimization trap. (a) Single obstacle. (b) Multiple obstacles.

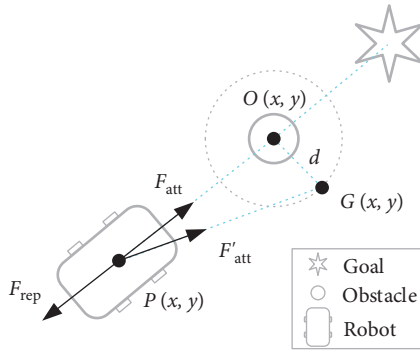


FIGURE 3: Triangle navigation method in single obstacle.

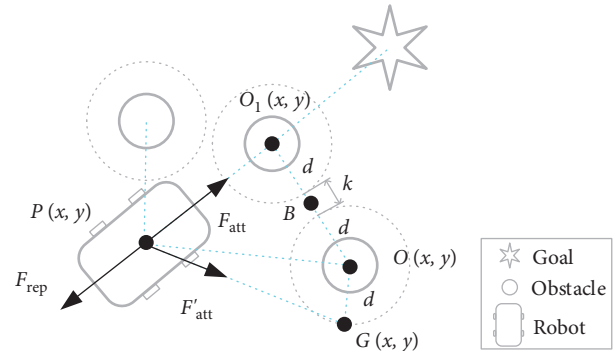


FIGURE 4: Triangle navigation method in multiple obstacles.

3.2.2. *Multiple Obstacles.* When the mobile robot encounters multiple obstacles and the joint force is zero, the robot falls into the local optimum and oscillates back and forth or stops. It needs to provide extra force to make the mobile robot escape from the local optimum. There are two solutions: the first is to pass through point B in the middle of multiple obstacles, and the second is to pass through G point, the outermost point of multiple obstacles, Figure 4 shows a schematic diagram of the two methods.

As shown in Figure 4, $O(x, y)$ and $O_1(x, y)$ are the coordinates of obstacles, and B is the midpoint of O and O_1 . The first method is to determine whether the length of k is greater than the width of the vehicle body to judge whether the mobile robot can pass through safely. If the condition is true, the guidance point B is calculated, and the local optimum is escaped through the additional attraction of point B . If the first method is not feasible, the second method is adopted, namely, the triangulation method. The guide point G is determined at the outermost periphery of the multiple obstacles, and the local optimum is escaped through the attraction force generated by the G point. According to the known obstacle coordinates $O(x, y)$ and the robot's current position coordinates $P(x, y)$, the coordinates of the guiding point $G(x, y)$ can be obtained by formula (7).

3.3. *Improved Repulsion Force Function.* According to the attraction force and repulsion force of classic APF formulas (3) and (4), the closer the mobile robot to the target point is, the less attractive force it receives. The closer the robot to an obstacle is, the greater repulsion force it receives. Figure 5

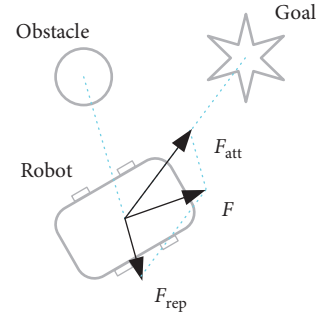


FIGURE 5: Schematic diagram of target unreachable.

shows the force analysis diagram of the target unreachable of the mobile robot.

Figure 5 shows how the mobile robot approaches the goal position when there is an impediment nearby, and the repulsive force F_{rep} it receives is substantially bigger than the attracting force F_{att} . It is unable to reach the goal location and oscillates near it.

The repulsion function is optimized, and the distance q_g between the mobile robot and the target point is incorporated as an adjustment factor, in order to tackle the problem of unreachable targets in the classical APF. The attractive force model F_{att1} is established to enhance the attractiveness of the target and ensure the attractive force received by the mobile robot near the target point is much greater than the repulsive force, so that the robot moves to the target point.

The optimized repulsion force function is as follows:

$$F_{\text{rep}} = \begin{cases} F_{\text{rep}1} + F_{\text{rep}2}, & 0 \leq q_{\text{obs}} \leq d_{\text{obs}}, \\ 0, & q_{\text{obs}} > d_{\text{obs}}, \end{cases} \quad (8)$$

where $F_{\text{rep}1}$ is the repulsion force component, direction from the obstacle to the mobile robot, and $F_{\text{att}1}$ is the attractive force component, direction from the mobile robot to the target point.

$F_{\text{rep}1}$ and $F_{\text{att}1}$ specific expressions are as follows:

$$\begin{cases} F_{\text{rep}1} = \sigma \left(\frac{1}{q_{\text{obs}}} - \frac{1}{d_{\text{obs}}} \right) \frac{q_g}{q_{\text{obs}}^2} \cdot \vec{q}_{\text{obs}}, \\ F_{\text{att}1} = k \cdot \sigma \left(\frac{1}{q_{\text{obs}}} - \frac{1}{d_{\text{obs}}} \right)^2 q_{\text{obs}} \cdot \vec{q}_g, \end{cases} \quad (9)$$

where k is the scale factor.

After optimizing the repulsion function, the received force of the mobile robot near the target point is shown in Figure 6.

In the repulsion force function (8), the repulsion force F_{rep} is composed of two components $F_{\text{rep}1}$ and $F_{\text{att}1}$. The target distance factor q_g is introduced, so that when the mobile robot approaches the target point, the repulsive force $F_{\text{rep}1}$ component gradually decreases, and the attractive force $F_{\text{att}1}$ component gradually increases, so that the mobile robot moves quickly to the target point. When the mobile robot reaches the target position, q_g becomes zero, and the joint force F acting on the mobile robot becomes zero as well, ensuring that the mobile robot reaches the target point stably and solving the problem of an unreachable target.

4. Simulations

In order to verify the effectiveness of the proposed IAPF model, MATLAB 2018b was used to simulate and analyse the path planning of the classic APF method and the IAPF method. The size of the simulation plane is $13 \text{ m} \times 13 \text{ m}$, and the system simulation parameter settings are listed in Table 1.

4.1. Simulation Analysis of Adaptive Step Length Adjustment. The classical APF method adopts the equal step path planning strategy, which is not suitable for the complex unknown environment and has met the problems of long system operation time and low path planning efficiency. The adaptive step length adjustment strategy is established and adopted in the improved algorithm, which gets the number and position of obstacles around the robot from the real-time scanning data of radar and automatically adjusts the forward step length of the mobile robot, as shown in Figure 7.

Figure 7(a) shows the classical path planning, which throughout adopts the equal-step path planning. Figure 7(b) shows an improved algorithm for path planning, and the density degree of the red dots in the curve depends on the step length of the path planning points. When there are many obstacles nearby, the robot planning step length decreases; that is, the moving speed decelerates, which reduces the probability of robot collision. Conversely, when there are

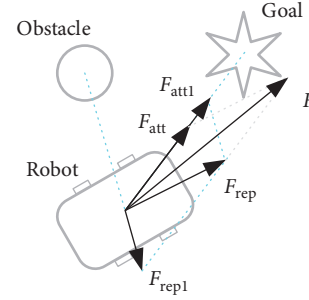


FIGURE 6: Optimized repulsion force function.

TABLE 1: Parameter setting.

Name	Symbol	Value
Attractive coefficient	μ	11
Repulsion coefficient 1	σ	3
Repulsion coefficient 2	k	2
Obstacle influence distance (m)	d_{obs}	1.5
Vehicle width (m)	$width$	0.8
Vehicle length (m)	$length$	1
Step length (m)	T_step	0.1
Number of cycles	c_{max}	1000
Starting position (m)	P_0	(0, 0)
Target location (m)	P_g	(12, 12)

fewer obstacles nearby, the robot planning step length increases, that is, to accelerate the moving speed, reduce the number of planning points, and improve the efficiency of path planning.

The specific algorithm comparison data are listed in Table 2. The IAPF algorithm has greatly improved the performance of the classical APF algorithm, the system planning efficiency has increased by 44.1%, the target convergence speed has increased by 26.3%, and the data calculated are listed in Table 2.

4.2. Local Optimal Simulation Analysis

4.2.1. Single Obstacle Situation. For the classic APF method, when the joint force of a single obstacle is zero, the robot loses the force of the potential field and loses the next planning path, so the robot stops moving. The simulation result is shown in Figure 8. Figure 8(a) depicts the robot being stuck at a local optimum. Under the potential field distribution, the robot is imprisoned in a local minimum, as shown in Figure 8(b). The coordinates of the minimum point are (5.62, 5.62). At this time, the mobile robot has a potential energy of 115.2 J.

For the IAPF method, when the robot falls into the local optimal state, the triangulation navigation method is started to generate a guide point. The guide point provides the attractive direction to help the mobile robot escape the local optimal state. The simulation result is shown in Figure 9. The improved model enables the mobile robot to overcome the local minimum and plan the destination path successfully.

Table 3 lists the simulation results for a single obstacle. The classical APF method falls into the local optimum, the robot stops moving, and the number of iterations is infinite.

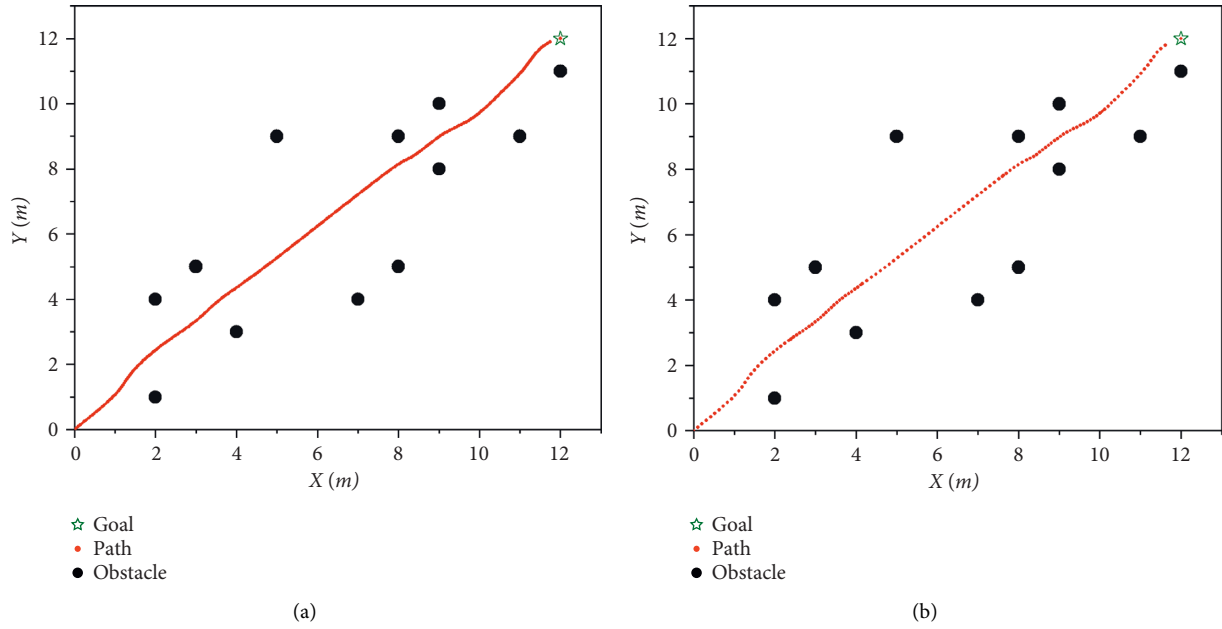


FIGURE 7: Simulation analysis of adaptive step length adjustment. (a) Classical APF algorithm. (b) IAPF algorithm.

TABLE 2: Algorithm comparison simulation data.

	Simulation time (s)	Number of iteration (s)	Planning efficiency* ¹ (improved)	Target convergence speed* ² (improved)
Classical APF method	0.1367	186		
IAPF method	0.0765	137	44.1%	26.3%

Note: *1 planning efficiency = | (simulation time of the IAPF method – imulation time of the classical APF method) | /simulation time of the classical APF method. *2 target convergence speed = | (number of iterations of the IAPF method – number of iterations of the classical APF method) | /number of iterations of the classical APF method.

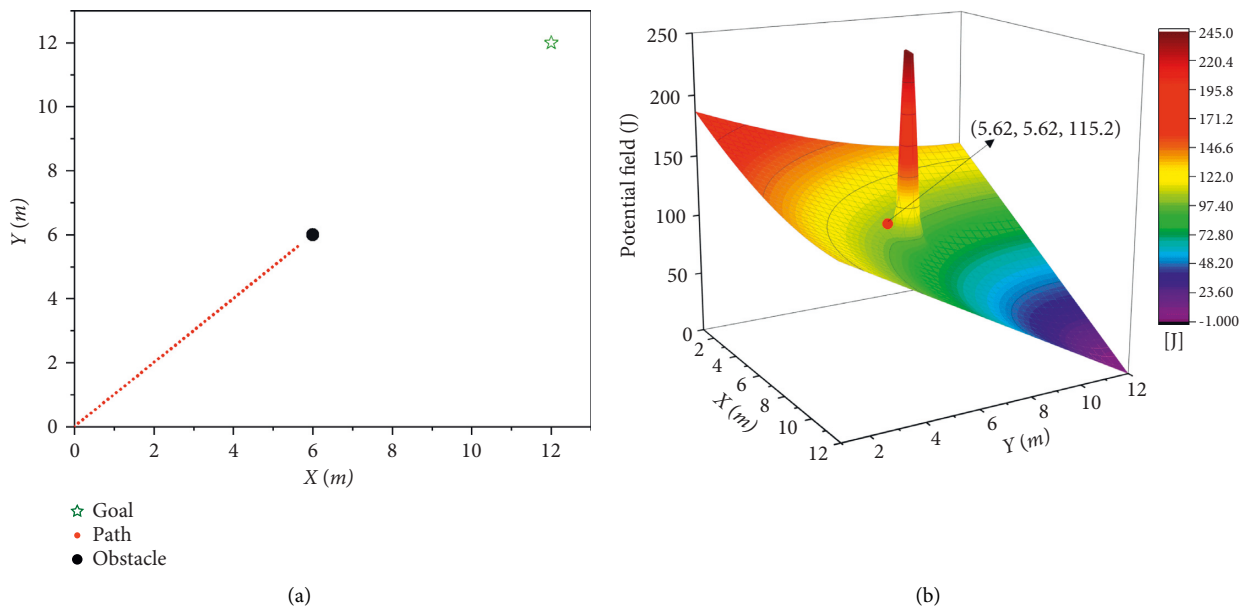


FIGURE 8: Simulation results of classical APF on single obstacle. (a) Trapped in local optimum. (b) Local most dominant field distribution.

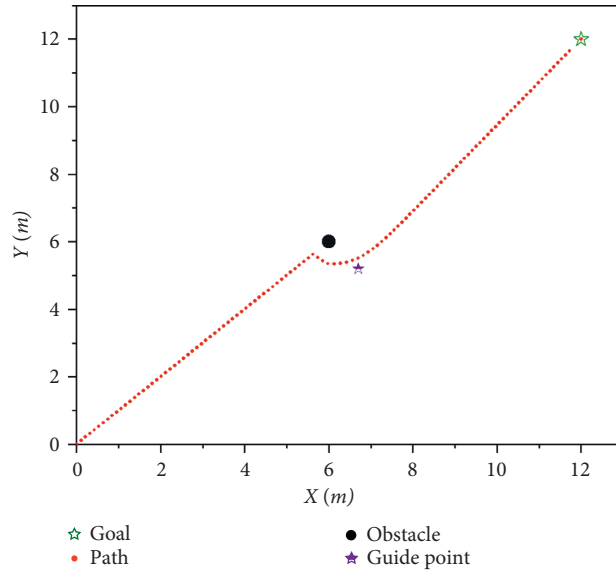
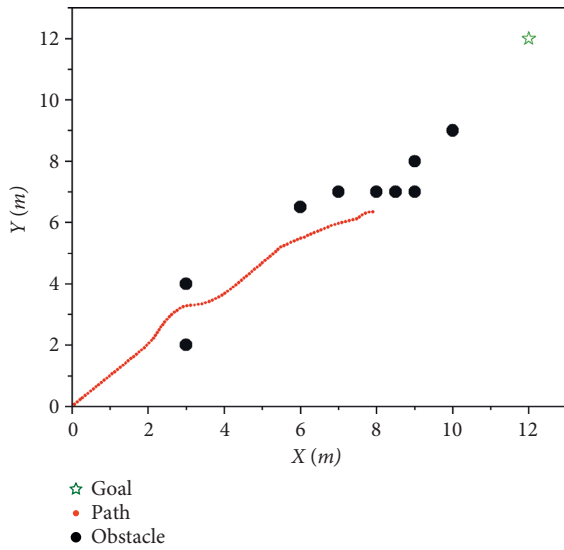


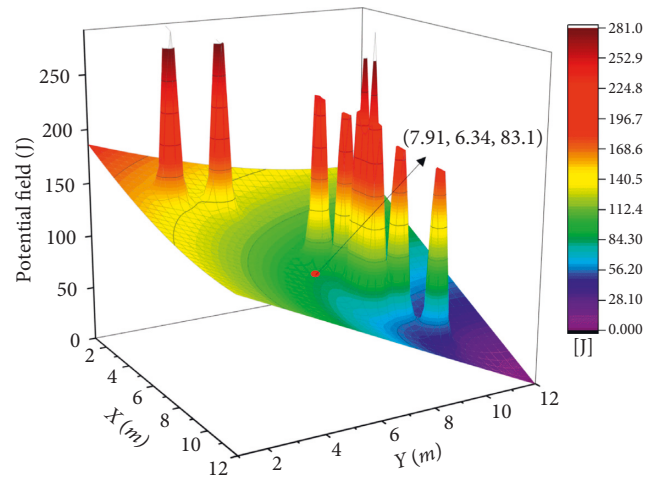
FIGURE 9: Simulation results of IAPF on single obstacle.

TABLE 3: Local optimal simulation results of a single obstacle.

Algorithm	Obstacle	Local optimum	Guidance point	Number of iterations
Classical APF method	(6, 6)	(5.62, 5.62)	Nothing	∞
IAPF method	(6, 6)	(5.62, 5.62)	(6.7, 5.2)	112



(a)



(b)

FIGURE 10: Simulation results of APF method on multiobstacles. (a) Trapped in local optimum. (b) Potential field distribution in local optimum.

The IAPF method solves the local optimal problem and reaches the target point smoothly. The whole process is iterated 112 times, with high efficiency and high speed.

4.2.2. Multiple Obstacles Situation. In the case of multiple obstacles and complex unknown environments, the mobile robot is easy to fall into the local optimal state, as

shown in Figure 10. The robot is caught in local optimization, as shown in Figure 10(a). In Figure 10(b), it can be seen that the robot is at the local minimum point (7.91, 6.34). At this time, the potential energy of the mobile robot is 83.1 J.

When the mobile robot is in the local optimal state, the triangle navigation method of the IAPF model is used to establish the guidance point, which helps the robot

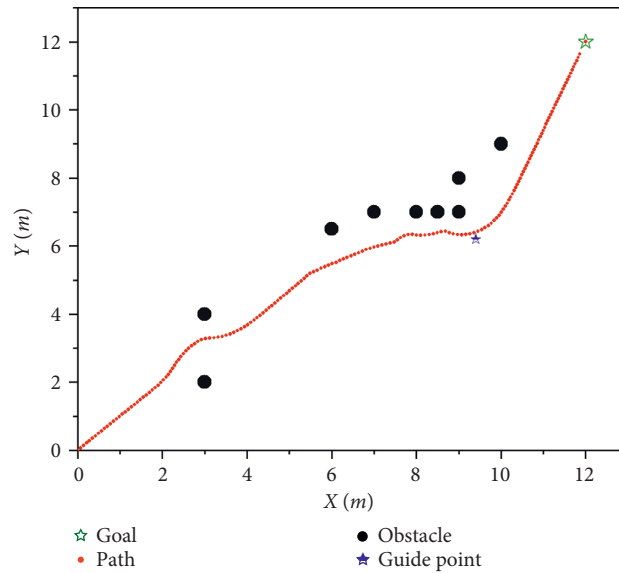
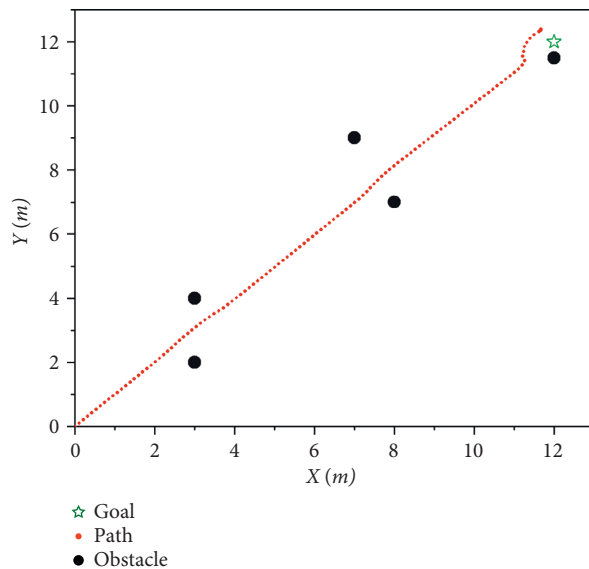


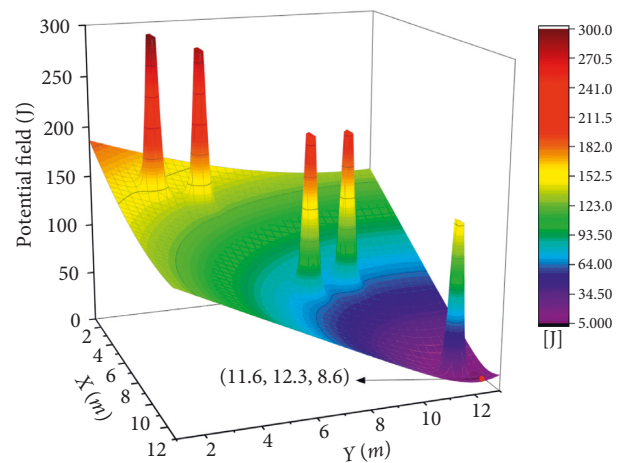
FIGURE 11: Simulation results of IAPF method with multiple obstacles.

TABLE 4: Local optimal simulation results of multiple obstacles.

Algorithm	Obstacles	Local optimum	Guidance point	Number of iterations
APF	(3, 2), (3, 4), (6, 6.5), (7, 7), (8, 7), (8.5, 7), (9, 7), (9, 8), (10, 9)	(7.91, 6.34)	Nothing	∞
IAPF	Dittos	(7.91, 6.34)	(9.4, 6.2)	180



(a)



(b)

FIGURE 12: Simulation results of the classic APF method. (a) Target unreachable. (b) Potential field distribution condition of target unreachable.

successfully plan the path to the destination, and the path is smooth, as shown in Figure 11.

The simulation results of multiple obstacles are listed in Table 4. The APF method falls into the local optimum, the robot stops moving, and the number of iterations is infinite. The IAPF method solves the local optimal problem, and the

whole process is iterated by 180 times, achieving fast convergence.

4.3. Target Unreachable Simulation Analysis. When obstacles are encountered near the target, the problem of target

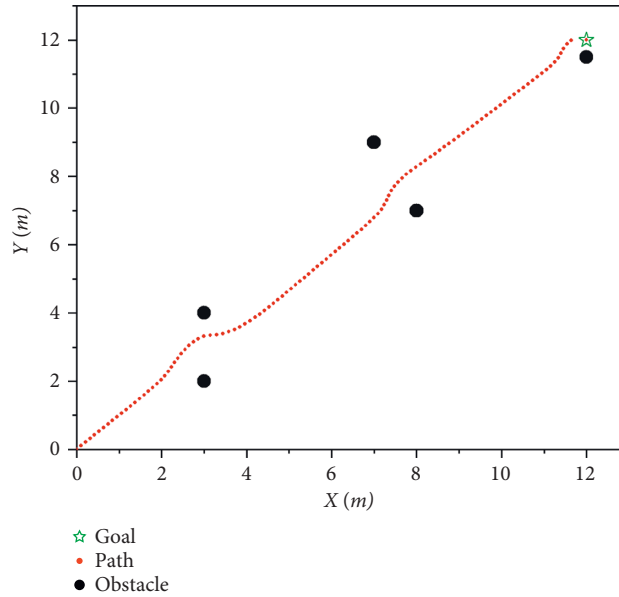


FIGURE 13: Simulation results of IAPF method.

TABLE 5: Simulation results of target unreachable.

Algorithm	Obstacles	Stop point	Number of iterations
APF	(3, 2), (3, 4), (7, 9), (8, 7) (12, 11.5)	(11.6, 12.3)	∞
IAPF	Dittos	(12, 12)	118

unreachable will occur by the APF method, as shown in Figure 12. Figure 12(a) shows the robot coming to a halt near the target spot. The repulsive force is seen near the target point in Figure 12(b), and the robot is unable to approach the target point directly, stopping at the coordinates (11.6, 12.3). At this time, the mobile robot has a potential energy of 8.6 J.

By improving the repulsion force model and optimizing the distance between the mobile robot and the target object into the repulsion function, the problem can be solved successfully. As shown in Figure 13, the robot overcomes the influence of repulsion and successfully reaches the endpoint.

The parameters of the simulation results of the target unreachable problem are listed in Table 5. The APF method cannot reach the target point, and the iteration times are infinite. The IAPF method reaches the target point after 118 iterations.

4.4. Comparative Simulation Analysis. According to the improved algorithm and the classical algorithm, several simulation experiments have been carried out, and the simulation is shown in Figure 14. Compared with the classical algorithm, the improved algorithm has a smoother path, shorter planned path, and faster convergence speed. Table 6 lists that the modified algorithm’s average path planning efficiency has increased by 42.8%, while the average

path length has decreased by 8.6%. The target’s average convergence speed has improved by 26.1%.

5. Experiments

To test the viability of the suggested real-time planning algorithm, it is used to plan the paths of mobile robots in unknown surroundings in order to obtain the defined target information without colliding. The host is a Jetbot mobile robot equipped with XR-Lidar S1 radar, and the slave is a notebook computer with a processor Intel Core i5-6300 and running memory of 16 GB. In the ROS Kinetic system of Ubuntu16.04, the surrounding environment information is obtained through the corresponding sensors for two-dimensional map construction and feasible path planning. According to the size of the prototype, a 6 * 8 m ground environment was selected for verification, and several cardboard boxes were placed as obstacles in the environment. The specific scenario is shown in Figure 15.

The Jetbot mobile robot is started, the Linux is opened on the computer, and the ROS system is loaded to enable the mobile robot to communicate with the computer. The mobile platform collects surrounding obstacle data through radar and odometer and transmits the collected data to the computer. The computer calls the gmapping function package to model the actual environment map. The mobile

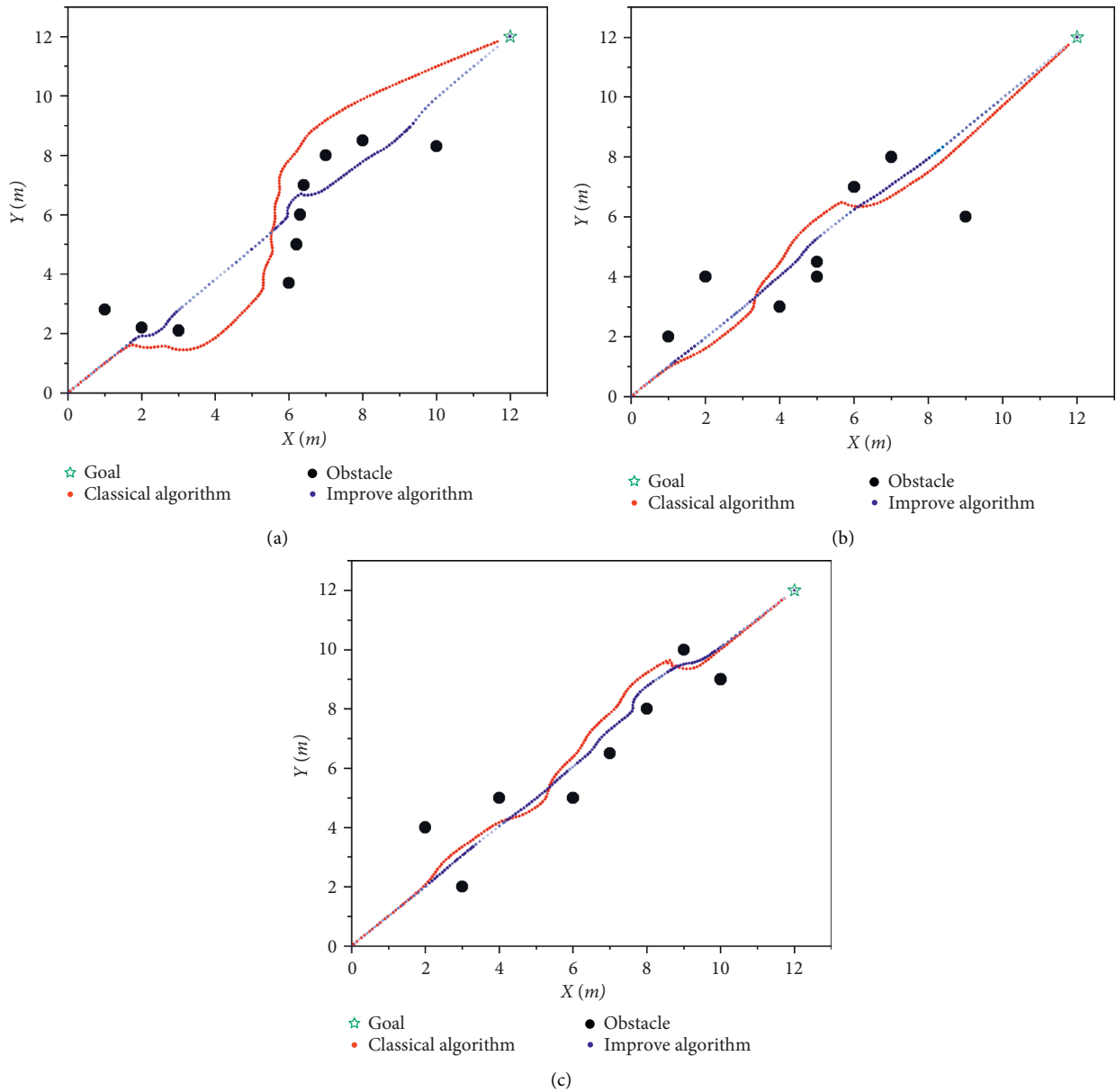


FIGURE 14: Algorithm simulation comparison. (a) Simulation one. (b) Simulation two. (c) Simulation three.

TABLE 6: Algorithm comparison on simulation data.

		Simulation time (s)	Path length (m)	Number of iterations	Planning efficiency (improved)	Path length* ¹ (decreased) (%)	Target convergence speed (improved)
Simulation one	APF	0.1234	19.2	186	44.6	10.4	29.1
	IAPF	0.0683	17.2	132			
Simulation two	APF	0.1354	18.7	174	37.2	8.5	27.0
	IAPF	0.0853	17.1	127			
Simulation three	APF	0.1172	18.6	183	46.8	6.9	22.4
	IAPF	0.0723	17.3	142			
Average planning efficiency (increased)						42.8%	
Average path length (decreased)						8.6%	
Average convergence speed (increased)						26.1%	

Note:*1 path length: $|\text{path length of IAPF} - \text{path length of APF}| / \text{path length of APF}$.

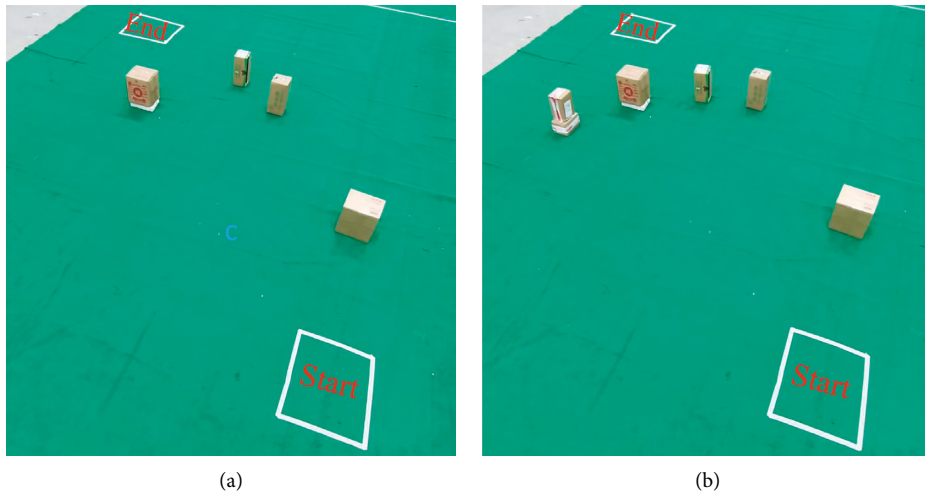


FIGURE 15: Test site. (a) Scene 1. (b) Scene 2.

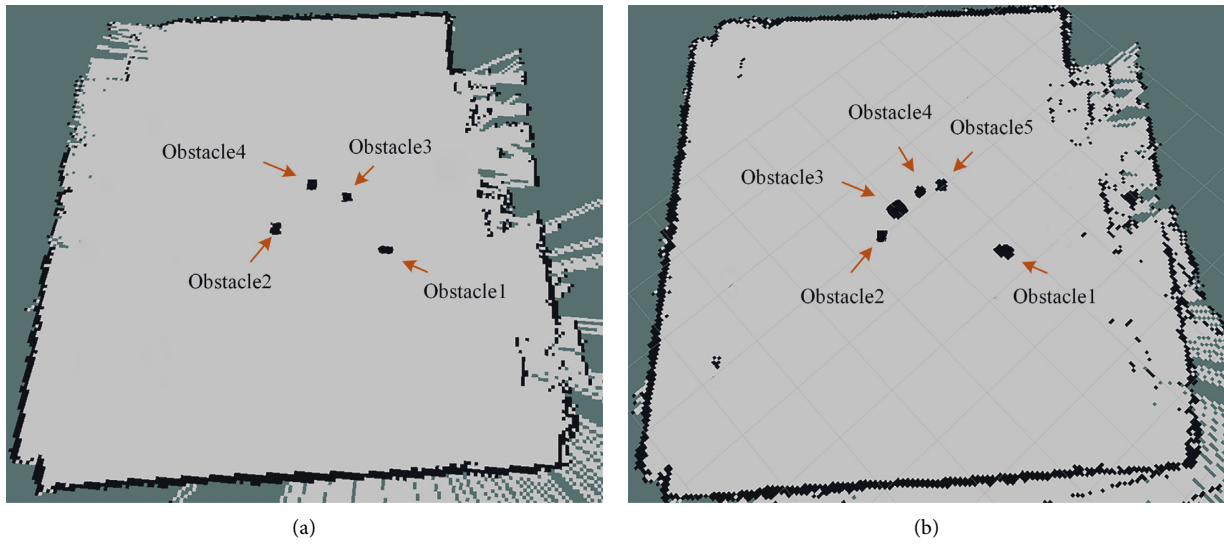


FIGURE 16: Raster map. (a) Scene 1 mapping. (b) Scene 2 mapping.

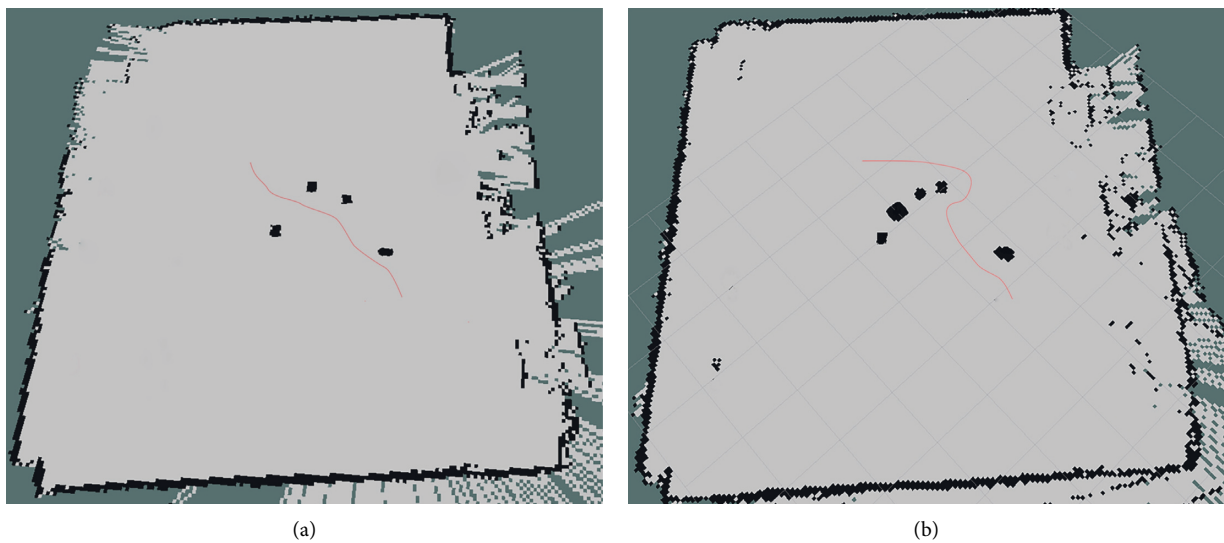


FIGURE 17: Improved algorithm navigation path map. (a) Scene 1 path planning. (b) Scene 2 path planning.

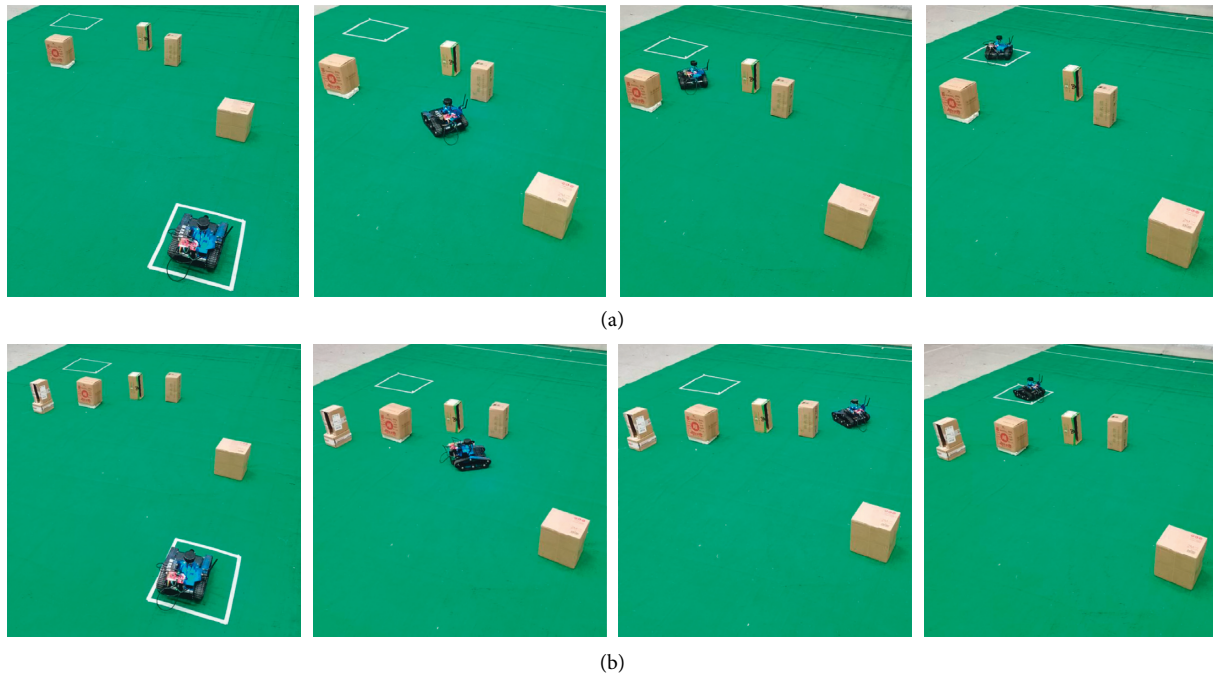


FIGURE 18: Physical test. (a) Scene 1 test. (b) Scene 2 test.

robot scans the actual environment to obtain a grid map, as shown in Figure 16.

The improved algorithm is used as a global planner in the ROS system in the form of a plug-in, and the parameters of the experimental platform are adjusted to write the launch file. The yaml file is loaded through rosparam to configure the platform parameters, the starting pose and target pose are set on the rviz visualization interface, and a global path is planned in the grid map. The path is shown in Figure 17. It can be seen from the path planning in the grid map that the improved algorithm successfully planned a feasible path with a smoother trajectory, which verified the feasibility of the improved artificial potential field algorithm.

The actual operation result of the ROS mobile platform in the ground environment is shown in Figure 18.

6. Conclusions and Future Work

Aiming at the problems existing in the application of classical APF method for mobile robots, a path planning model based on IAPF is designed. The simulation results show that the average path planning efficiency of the improved model increases by 42.8%, the average path length decreases by 8.6%, and the average target convergence speed increases by 26.1%, which verifies the effectiveness and accuracy of the IAPF.

A novel triangle navigation method is designed, and the guiding point is established to solve the problem that the mobile robot falls into local optimum. Adaptive step length adjustment strategy is designed, and step length is reasonably planned according to the number of obstacles, so as to improve the operation efficiency of the algorithm. A new target attractive force model based on obstacle distance is

built to improve the convergence speed of the target, and a target factor is added to optimize the repulsion function, which solves the problem of unreachable targets.

The research described in the study was completed in a static environment with certain limitations and did not consider the presence of dynamic obstacles. Therefore, the dynamic obstacle environment will be studied in the future to realize the real-time obstacle avoidance function of the mobile robot. In addition, several aspects of the works in this study remain to be further investigated: first, the paths are deredundantly processed to get shorter paths. Second, the B spline curve strategy is introduced to smooth the paths.

Data Availability

The data used to support the findings of this study are available from the corresponding author upon request.

Conflicts of Interest

The authors declare that they have no conflicts of interest.

Authors' Contributions

Conceptualization, methodology, software, and data analysis are performed by Tiezheng Guo; formal analysis, investigation, validation, and writing—original draft preparation are performed by Jie Wang; project administration and funding acquisition are performed by Zhiming Wang; technical guidance, review, and editing are performed by Wei Chen and Guojun Chen; experimental platform construction and data collection are performed by Shishi Zhang. All authors have read and agreed to the published version of the manuscript.

Acknowledgments

This research work was supported by the Jiangsu Provincial Agricultural Science and Technology Independent Innovation Fund Project (grant number: CX(21)1007), the Open Project of the Zhejiang Provincial Key Laboratory of Crop Harvesting Equipment and Technology (grant numbers: 2021KY03 and 2021KY04), the Jiangsu Provincial Key Research and Development Project (grant number: BE2021016-5) and the Jiangsu Province Postgraduate Research and Practice Innovation Program (grant numbers: SJCX21_0933 and SJCX21_0940).

References

- [1] K. Li, Q. Hu, and J. Liu, "Path planning of mobile robot based on improved multi-objective genetic algorithm," *Wireless Communications and Mobile Computing*, vol. 2021, Article ID 8836615, 2021.
- [2] Z. Hong, W. Du, and H. Wang, "Design and implementation of path planning for wheel-track hybrid mobile robot[J]," *Mobile Information Systems*, vol. 2022, Article ID 6418706, 2022.
- [3] X. Lai, J. H. Li, and J. Chambers, "Enhanced center constraint weighted a * algorithm for path planning of petrochemical inspection robot[J]," *Journal of Intelligent and Robotic Systems*, vol. 102, no. 4, pp. 1–15, 2021.
- [4] J. F. Duhé, S. Victor, and P. Melchior, "Contributions on artificial potential field method for effective obstacle avoidance," *Fractional Calculus and Applied Analysis*, vol. 24, no. 2, pp. 421–446, 2021.
- [5] Y. V. Pehlivanoglu and P. Pehlivanoglu, "An enhanced genetic algorithm for path planning of autonomous UAV in target coverage problems," *Applied Soft Computing*, vol. 112, Article ID 107796, 2021.
- [6] Y. Pan, Y. Yang, and W. Li, "A deep learning trained by genetic algorithm to improve the efficiency of path planning for data collection with multi-UAV," *IEEE Access*, vol. 9, pp. 7994–8005, 2021.
- [7] M. D. Phung and Q. P. Ha, "Safety-enhanced UAV path planning with spherical vector-based particle swarm optimization," *Applied Soft Computing*, vol. 107, Article ID 107376, 2021.
- [8] X. h Liu, D. Zhang, J. Zhang, T. Zhang, and H. Zhu, "A path planning method based on the particle swarm optimization trained fuzzy neural network algorithm," *Cluster Computing*, vol. 24, no. 3, pp. 1901–1915, 2021.
- [9] U. Orozco-Rosas, O. Montiel, and R. Sepúlveda, "Mobile robot path planning using membrane evolutionary artificial potential field," *Applied Soft Computing*, vol. 77, pp. 236–251, 2019.
- [10] A. Azzabi and K. Nouri, "An advanced potential field method proposed for mobile robot path planning," *Transactions of the Institute of Measurement and Control*, vol. 41, no. 11, pp. 3132–3144, 2019.
- [11] S. M. H. Rostami, A. K. Sangaiah, J. Wang, and X. Liu, "Obstacle avoidance of mobile robots using modified artificial potential field algorithm," *EURASIP Journal on Wireless Communications and Networking*, vol. 1, pp. 70–19, 2019.
- [12] J. Batista, D. Souza, J. Silva et al., "Trajectory planning using artificial potential fields with metaheuristics," *IEEE Latin America Transactions*, vol. 18, no. 05, pp. 914–922, 2020.
- [13] J. H. Jung and D. H. Kim, "Local path planning of a mobile robot using a novel grid-based potential method," *International Journal of Fuzzy Logic and Intelligent Systems*, vol. 20, no. 1, pp. 26–34, 2020.
- [14] M. Pashna, R. Yusof, Z. H. Ismail, T. Namerikawa, and S. Yazdani, "Autonomous multi-robot tracking system for oil spills on sea surface based on hybrid fuzzy distribution and potential field approach," *Ocean Engineering*, vol. 207, Article ID 107238, 2020.
- [15] Y. Chen, G. Bai, Y. Zhan, X. Hu, and J. Liu, "Path planning and obstacle avoiding of the USV based on improved ACO-APF hybrid algorithm with adaptive early-warning," *IEEE Access*, vol. 9, pp. 40728–40742, 2021.
- [16] Y. Shin and E. Kim, "Hybrid path planning using positioning risk and artificial potential fields," *Aerospace Science and Technology*, vol. 112, Article ID 106640, 2021.